ISIJ International, Vol. 43 (2003), No. 9, pp. 1431–1437

Precipitate Dissolution and Grain Growth in the Heat Affected Zone of HSLA-100 Steel

M. SHOME, D. S. SARMA,[1)] O. P. GUPTA[2)] and O. N. MOHANTY

R&D and Scientific Services Division, Tata Steel, Jamshedpur 831007, India. E-mail: mshome@tatasteel.com
1) Department of Metallurgical Engineering, Institute of Technology, Benaras Hindu University, Varanasi 221005, India. E-mail: dssarma@banaras.ernet.in 2) Department of Mechanical Engineering, Indian Institute of Technology, Kharagpur 721302, India. E-mail: opgupta@mech.iitkgp.ernet.in

(*Received on October 11, 2002; accepted in final form on April 1, 2003*)

An attempt has been made to predict the dissolution of Nb(CN) precipitates in the heat affected zone (HAZ) of a Nb containing HSLA-100 steel. An invariant size approximation model along with existing solubility product data have been applied to continuous heating and cooling situation to ascertain the kinetic strengths from heat input–peak temperature conditions at which dissolution of precipitates take place. Peak temperatures beyond which precipitates rapidly dissolve and cause grain growth have been identified, and they are in consonance with the austenite grain growth data.

KEY WORDS: welding, heat affected zone, niobium carbonitride, HSLA-100, heat input, precipitate dissolution, grain growth, kinetic strength.

1. Introduction

Niobium carbo–nitride precipitates in Nb-containing steels prevent grain growth during the re-heating process. Austenite grain growth as a result of precipitation dissolution in these steels has been extensively investigated[1)] under isothermal conditions. The thermal stability of the precipitates depends primarily on the Nb content; this can be estimated fairly accurately from the existing solubility product relationships.

Studies conducted under isothermal conditions[2–4)] show a resistance to normal grain growth at low temperatures as the precipitates exert pinning effect on the austenite grain boundary. With increasing temperature the precipitates gradually dissolve in austenite losing their pinning effect. In the heat affected zone (HAZ) of welds, dissolution of the precipitates takes place in regions experiencing temperatures higher than the equilibrium dissolution temperature of precipitates leading to grain coarsening. Ashby *et al*. and Ion *et al*.[5,6)] have provided some insight into the dissolution limits for NbC particles in micro-alloyed steels.

The grain growth kinetics in the HAZ can be better explained by tracking the change in the size of the dissolving particles as a function of the weld thermal cycle. In view of the difficulty in carrying out precise precipitate measurements experimentally, Anderson *et al*.[7)] have suggested a simplified precipitation dissolution model for non-isothermal conditions based on the Whelan–Agren's invariant size approximation solution.[8,9)] The present investigation has been carried out to evaluate the dissolution kinetics of niobium carbo–nitride [$Nb(C_xN_{1-x})$] precipitates using the Whelan–Agren model and relate it to the observed grain growth in the weld-HAZ of a Nb containing HSLA-100 steel.

2. Experimental Procedure

Experiments were carried out to simulate weld-HAZ in a Gleeble-1500 thermo–mechanical simulator. The simulated temperature–time cycles imposed on the samples were governed by Rykalin's thick plate (3D) equation, which is given by[10,11)]:

$$T=\frac{q}{2\pi\lambda t}\exp\left(\frac{r^2}{4at}\right) \quad \text{.....(1)}$$

where q is the welding heat input, λ is the thermal conductivity, a is the thermal diffusivity, and r is the radial distance from the weld center. The radial distance r in Eq. (1) is given as:

$$r=\sqrt{\frac{2q}{T_p c\rho\pi e}} \quad \text{.....(2)}$$

where T_p is the peak temperature, c is the specific heat capacity, and ρ is the density of the steel. For HSLA-100 steels c was taken as 0.5 J/gm·°C, λ as 0.4 J/cm·sec°K, a as 0.102 cm^2/s, ρ as 7.8 gm/cm^3 and e (=2.718) is the base of logarithm.

The study was carried out on a HSLA-100 steel, chemistry of which is given in **Table 1**. Weld simulations were carried out with heat inputs of 10 kJ/cm and 40 kJ/cm, with peak temperatures of 900°C to 1 400°C [at intervals of 100°C] in round grooved samples, prepared from plates.

Table 1. Composition of HSLA-100 steel (mass %).

HSLA	C	Mn	Si	S	P	Cu	Ni	Cr	Mo	Al	Nb	N (ppm)
100	0.04	0.84	0.26	0.006	0.007	1.58	3.55	0.55	0.59	0.03	0.029	128

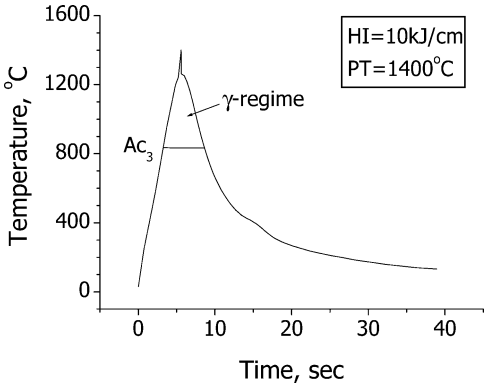

Fig. 1. Typical thermal profile of a HAZ simulation.

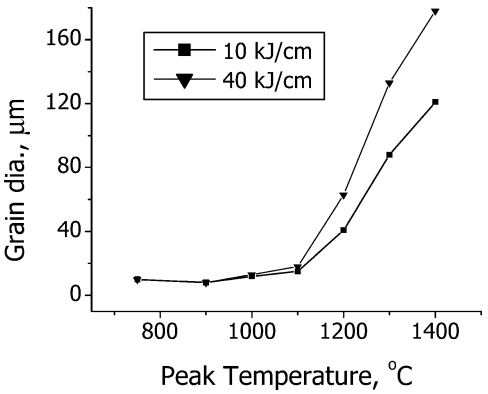

Fig. 3. Grain growth in the HAZ of HSLA-100 steel as a function of heat input.

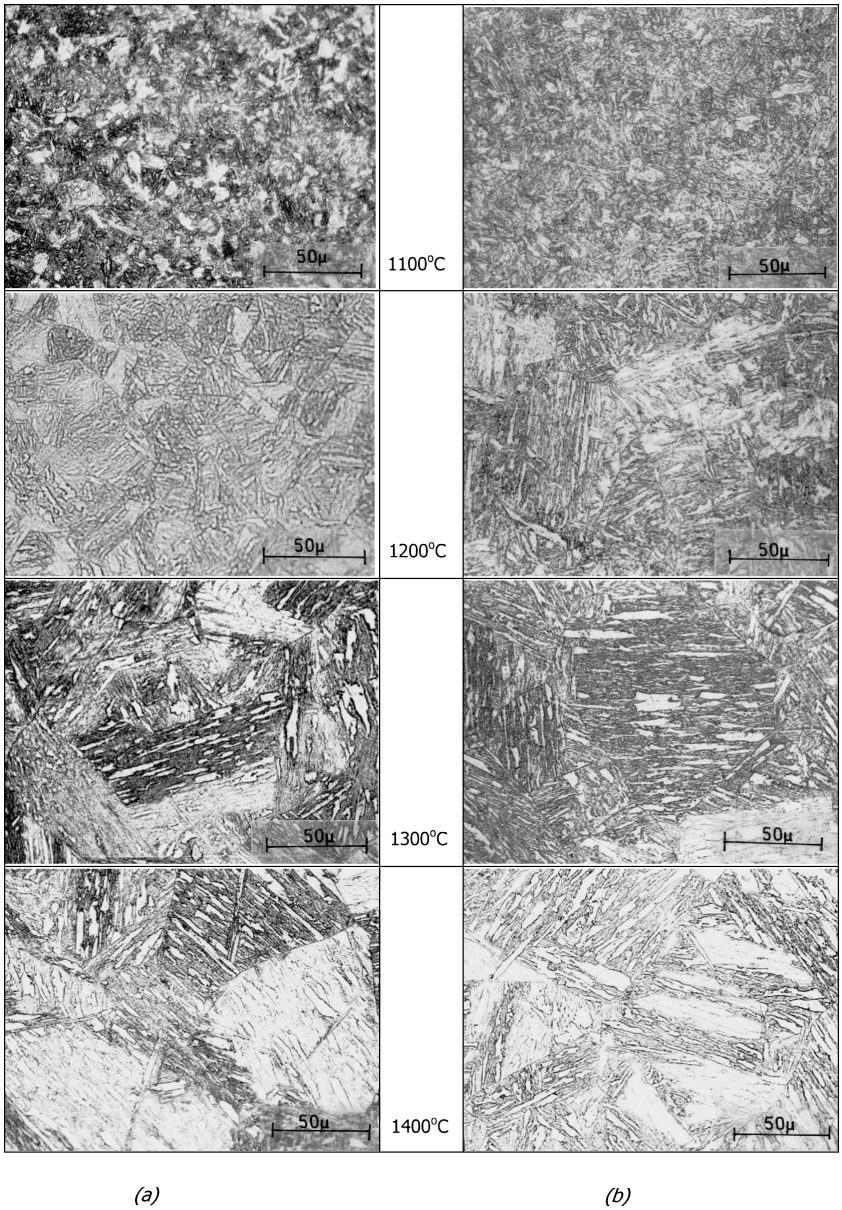

Fig. 2. Microstructure as a function of peak temperature in HAZ simulated HSLA-100 samples with heat input of (a) 10 kJ/cm and (b) 40 kJ/cm.

The simulation section represented a small cylinder of 6mm length and 6 mm diameter. A uniform heating rate of 200°C/s from room temperature to peak temperature was imposed on the sample. The cooling time between 800°C and 300°C (Δt_{8-3}) for 10 kJ/cm heat input was 10 s and for 40 kJ/cm heat input was 42 s. A typical thermal cycle is shown in **Fig. 1**.

Slices were cut from the center of the samples at the point of thermo-couple contact, polished and etched with 2% nital, then examined for microstructure. Additionally, a boiling solution containing 10 g CrO_3, 50 g NaOH, 1.5 g picric acid in 100 ml distilled water[12] was used for etching specific samples that were exposed to 900–1 100°C peak temperature. The mean lineal intercept length and individual grain intercept length were measured according to ASTM E112-96 method. Results have been reported in terms of grain diameter, which is 1.5 times the mean linear intercept value.

TEM observations were carried out to determine the precipitate type, size and its distribution, for peak temperatures of 1 100 and 1 200°C, for low heat input (fast cooled) and high heat input (slow cooled) structures. Foils for TEM observation were prepared from slices taken from the center of the samples, ground and thinned using a twinjet elec-

Table 2. Average cooling rates from PT to 800°C for two different heat inputs.

Heat Input, kJ/cm	Average cooling rate, °C/sec				
	PT=1000°C	PT=1100°C	PT=1200°C	PT=1300°C	PT=1400°C
10	107	126	146	164	192
40	24	30	37	45	51

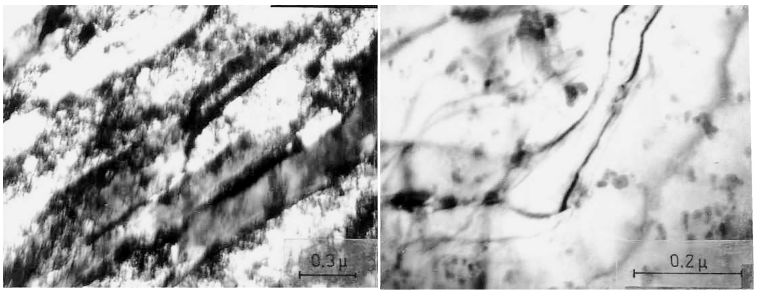

(a) (b)

Fig. 4. TEM micrographs of (a) lath martensite containing high dislocation density (b) Nb(CN) precipitates within martensite laths in HAZ (PT, 1 100°C; HI, 10 kJ/cm).

tropolishing unit with a solution containing 90% acetic acid and 10% perchloric acid, at 10°C with an operating voltage of 30 V. The TEM observations were performed at 120 kV.

3. Results

3.1. HAZ Thermal Cycle and Grain Size

The microstructures primarily consist of lath martensite and acicular ferrite as shown in **Fig. 2**. The micrographs also reveal the prior austenite grain size as a function of peak temperature (PT) and cooling rate. With heat inputs of 10 and 40 kJ/cm and peak temperatures of 1 100°C or below the grain growth is not significant. However, rapid grain growth is observed (**Fig. 3**) at peak temperatures beyond 1 100°C. The overall austenite regime in Fig. 1 depends on the heat input and peak temperature and is best represented by the area under the time-temperature curve corresponding to the Ac_3 temperature. The peak temperature and dwelling time of austenite determine the propensity of grain growth in the HAZ. Based on the formula[13], $Ac_3 = 910 - 203\sqrt{\%C} - 15.2(\%Ni) + 44.7(\%Si) + 31.5(\%Mo)$, the Ac_3 temperature calculated for HSLA-100 steel was found to be 846°C.

3.2. Precipitate Type and Size Estimation Using TEM

The average cooling rates within the high temperature austenite phase for two heat inputs and different peak temperatures are given in **Table 2**. The microstructure developed at peak temperature of 1 100°C with 10 kJ/cm heat input (HI) is shown in **Fig. 4**(a). It shows a typical lath martensite structure in the HAZ with high dislocation density. A large number of precipitates were observed within the individual laths and lath boundaries. Precipitates seen in several areas of the foil are shown in Fig. 4(b).

The microstructure developed with peak temperature of 1 100°C with 40 kJ/cm heat input is shown in **Fig. 5**(a). A large number of precipitates can be seen within the martensite laths. Selected area diffraction shows the presence of Nb(CN) precipitate; further confirmed by the dark field image in Fig. 5(b). The diameters of the particles vary between 100–300 Å, however the average is around 200 Å.

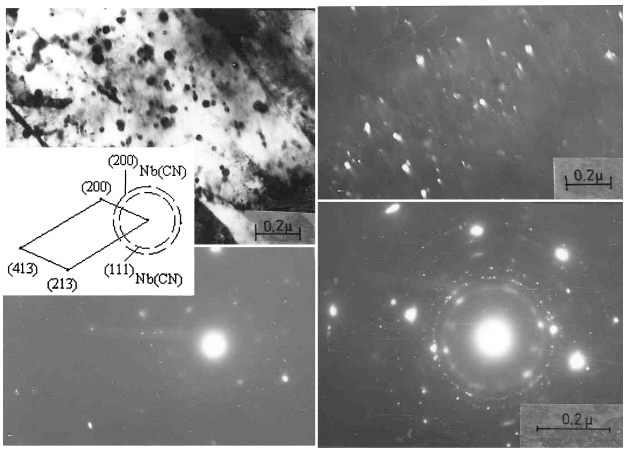

(a) (b)

Fig. 5. TEM micrographs showing (a) Nb(CN) precipitates with SAD pattern in [0$\bar{3}$1] orientation showing reflections of 111 and 200 rings, (b) DF image of precipitates with SAD pattern in [0$\bar{1}$2] orientation showing Nb(CN) reflections in HAZ (PT, 1 100°C; HI, 40 kJ/cm).

Specimens exposed to peak temperature of 1 200°C with 10 and 40 kJ/cm heat input (**Fig. 6**) also show a typical lath martensite structure with high dislocation density; these specimens though are free from any precipitates within the laths or lath boundaries. This clearly indicates that most of the Nb(CN) particles have dissolved.

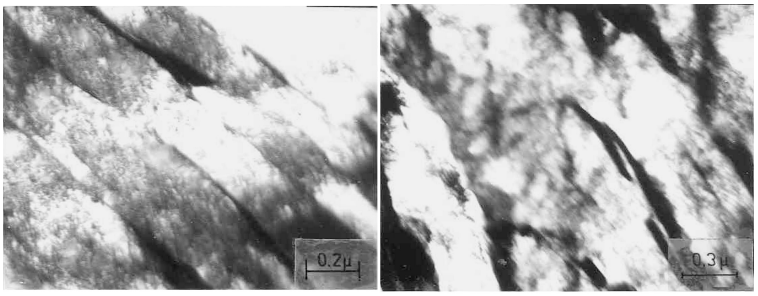

(a) (b)

Fig. 6. TEM micrographs of (a) lath martensite developed at PT, 1 200°C, HI, 10 kJ/cm, and (b) lath martensite developed at PT, 1 200°C; HI, 40 kJ/cm. The laths are free from any precipitates.

4. Application of the Whelan–Agren Model

4.1. Precipitate Dissolution under Isothermal Conditions

Whelan[8] developed an invariant size approximation model to obtain particle radius as a function of time, which was further modified by Agren[9] to describe the dissolution kinetics of small precipitates in steel during heating above Ac_3-temperature. Using this model the time required for complete dissolution of spherical precipitates can be obtained for an isothermal heat treatment.

4.2. Precipitate Volume Fraction Transformed under Non-isothermal Conditions

Anderson[7,11] obtained the volume fraction of precipitate f as a function of time by applying the Whelan–Agren model to continuous heating and cooling conditions, and is given as:

$$f = f_0\left(\frac{r}{r_0}\right)^3 = f_0\left\{1-\frac{2}{(r_0)^2}\int_{t_1}^{t_2}\alpha_{Nb}D_{Nb}dt\right\}^{3/2} \quad .....(3)$$

where f_0 is the initial precipitate volume fraction, r_0 is the original particle radius, D_{Nb} is the dimensionless supersaturation parameter, and D_{Nb} is the bulk diffusivity of Nb. The expression $2\int_{t_1}^{t_2}\alpha_{Nb}D_{Nb}dt$ in Eq. (3) is the kinetic strength of the thermal cycle for precipitate dissolution. The lower and upper integration limits refer to the time spent by the weld thermal cycle in the austenite region, i.e. from Ac_3 (846°C) to peak temperature, T_p, and down again to Ar_3. The dimensionless supersaturation value (α) is given by:

$$\alpha_{Nb} = C_i/C_p \quad .....(4)$$

C_i is the concentration of Nb in the austenite matrix/particle interface and C_p is the concentration of Nb in the precipitate. Using this modified approach, it is possible to determine the temperature at which a spherical precipitate would completely dissolve for a particular thermal cycle.

4.2.1. Inputs to the Model

As the equilibrium dissolution temperature for Nb(CN) in the present steel is calculated[14] to be 1 115°C, it may be assumed that no further precipitate growth takes place beyond 1 100°C and the dissolution process is dominant at this stage. Although a spectrum of precipitate sizes was observed in TEM, most precipitates were close to 200 Å diameter. Therefore for theoretical consideration the starting size of the precipitate for the dissolution model has been considered to be 200 Å diameter.

The C_i of Eq. (4) can be directly obtained from the solubility product k of $Nb(C_xN_{1-x})$ at different temperatures. The fraction of C and N in niobium-carbonitride precipitates for a given chemistry can be obtained from solubility product relations[14–17], and is given in Appendix I. For the given HSLA-100 chemistry, the carbonitride can be expressed as $NbC_{0.23}N_{0.77}$ for practically all temperatures in the austenite region.

The equilibrium concentration of Nb, C_i, at the particle/matrix interface (in mass%) and the concentration of the precipitate C_p can be estimated from the solubility product equation and is described in Appendix II. The concentrations C_i and C_p are combined to give the dimensionless supersaturation value (α) that is expressed as a function of the temperature, T, and is integrated over a time period using Eq. (3).

4.2.2. Prediction of the Model

The ratio of volume of precipitates remained to the initial volume of precipitate (f/f_0) as a function of peak temperature is obtained by inserting appropriate values of α and D_{Nb} [$5.9\times10^4\exp(-41256/T)$] in Eq. (3), and is expressed as:

$$f = f_0\left\{1-\frac{41654000}{r_0^2}\int_{t_1}^{t_2}\exp\left(-\frac{60510}{T}\right)dt\right\}^{3/2} \quad .....(5)$$

The extent of particle dissolution has been calculated in an iterative manner by numerical integration over the weld thermal cycle. The plot of volume fraction of precipitate as a function of peak temperature is given for two different heat inputs in Fig. 7.

The model predicts that the precipitate dissolution is completed in temperature cycles raised to 1 230°C with 10 kJ/cm heat input and 1 190°C with 40 kJ/cm heat input. The peak temperature at which maximum change of slope occurs has been obtained by extrapolating the straight portions of the dissolution curve. This temperature is 1 168°C for 10 kJ/cm heat input and 1 146°C for 40 kJ/cm heat input.

5. Discussion

The kinetics of the process suggest that the maximum temperature attained and dwelling time of the austenite phase should be related to the kinetic strength of the thermal cycle, which determines the extent of Nb(CN) dissolution in the matrix. As can be seen from Eq. (3) the kinetic strength depends largely on the diffusivity of Nb along the temperature cycle, and therefore it is larger for higher peak temperatures. The kinetic strength grows exponentially with the area between the thermal cycle and the Ac_3 line, and their relationship is given in Table 3 for different peak temperatures.

The results of the Whelan–Agren model shown in **Fig. 7** illustrates that the dissolution of the precipitates is prominent beyond 1 100°C peak temperature for both slow and fast cooling conditions. Likewise, the grain growth plots in Fig. 3 show that the grains grow rapidly at peak temperatures beyond 1 100°C. The distinction in behavior between the 10 kJ/cm and 40 kJ/cm situation is not visible in the absence of actual data on grain size corresponding to temperatures in the range of 1 100–1 200°C. As indicated by the dissolution curves (Fig. 7) it is possible that the precipitates remain fairly stable till 1 146°C for 10 kJ/cm heat input and 1 168°C for 40 kJ/cm heat input. Beyond this temperature significant reduction of precipitate size is expected, thereby preventing effective pinning of the austenite grain boundaries. This is amply demonstrated by the grain size values corresponding to the kinetic strength for each peak temperature (**Table 3**).

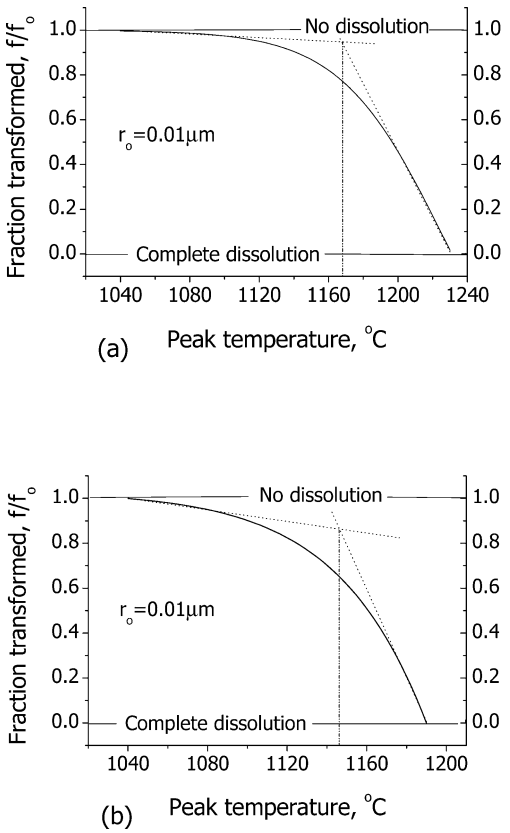

Fig. 7. Dissolution of Nb(CN) in the HAZ of HSLA-100 steel under (a) 10 kJ/cm heat input and (b) 40 kJ/cm heat input.

As can be seen from the micrographs (Figs. 2, 4, 5 and 6), there is a predominance of lath martensite with films of retained austenite between the laths in all the HAZ structures. This structure is a result of the fast cooling rate of welding. Dense precipitates, mostly around 200 Å are present in samples exposed to peak temperature of 1 100°C with heat inputs of 10 and 40 kJ/cm. This indicates that the precipitate size remains almost intact at 1 100°C even though it is close to the precipitation dissolution temperature of 1 115°C in this steel. Spanos[12] had earlier shown the stability of similar size Nb(CN) precipitates exposed to weld cycles with peak temperature of 900°C in the same steel. However, no information seems to be available on precipitate size or grain growth in literature for weld cycles covering temperatures between 900 and 1 400°C. The findings clearly demonstrate that the dissolution rate of the Nb(CN) precipitates was limited because of the lower kinetic strength of the thermal cycles at this temperature.

When the peak temperature was raised to 1 200°C with 10 kJ/cm heat input, most of the laths were free of precipitates and only a few showed faint precipitate rings. This implies that most of the precipitates within the lath or at the lath boundaries had dissolved and apparently not re-precipitated during cooling. In samples exposed to peak temperature of 1 200°C with a higher heat input (40 kJ/cm), no precipitates were observed in the resulting microstructure. This is because a higher peak temperature increased the diffusivity of Nb along the thermal path and the dwelling time of the re-transformed austenite, thereby enhancing the kinetic strength of the thermal cycle in the 40 kJ/cm heat input simulation.

Table 3. Relation between area under the thermal curve and kinetic strength for precipitate dissolution.

Peak Temp, °C	Heat Input					
	10kJ/cm			40kJ/cm		
	Area, °C.sec	Kinetic strength, μm^2	Av. grain dia, μm	Area, °C.sec	Kinetic strength, μm^2	Av. grain dia, μm
1100	433	2.33 x 10^{-6}	15	1319	6.49 x 10^{-6}	18
1200	744	4.33 x 10^{-5}	41	2118	1.18 x 10^{-4}	63
1300	1114	5.62 x 10^{-4}	88	2994	1.52 x 10^{-3}	123
1400	1537	5.49 x 10^{-3}	121	3814	1.43 x 10^{-2}	178

A fast heating rate (200°C/s) to a higher peak temperature provides the necessary degree of superheating to overcome the kinetic barrier required for dissolution to start. However, the bulk of the precipitate dissolution takes place during the cooling process in the high temperature domain, as the cooling rate is relatively slower. Thereby the precipitate dissolution process is enhanced with the increase in peak temperature and heat input.

The correlation between the theoretical results and the experimental findings suggest that the invariant size approximation model can be used with good effect to predict precipitate dissolution in HSLA-100 steels and thereby grain growth under continuous heating and cooling conditions.

6. Conclusion

The following can be concluded from the above study:

(1) The invariant size approximation model predicts that typical niobium carbonitride precipitates (~200 Å dia.) in the HAZ of HSLA-100 steel completely dissolves under temperature cycles with peak temperatures of 1 230 and 1 190°C for heat inputs corresponding to 10 and 40 kJ/cm respectively. The model also indicates that rapid dissolution of the precipitates takes place above 1 168°C peak temperature for 10 kJ/cm heat input and 1 146°C peak temperature for 40 kJ/cm heat input.

(2) The dissolution of precipitates as suggested by the model has been confirmed by TEM studies. A large number of fine Nb(CN) precipitates that were retained in the lath martensite structure exposed to thermal cycles with peak temperature of 1 100°C were almost absent in the structures of samples treated by the thermal cycles with peak temperature of 1 200°C and above.

(3) The instability of the precipitates and their dissolution with increasing peak temperature (beyond 1 100°C) and heat input was accompanied by rapid grain growth in the HAZ of HSLA-100 steels. The actual grain growth data *vis-à-vis* predictions of the precipitation dissolution model show good correlation.

ACKNOWLEDGEMENTS

The authors would like to acknowledge the financial support (Grant No. N00014-95-1-00015 [P4]) provided for this study jointly by the Department of Science and Technology, Govt. of India and the Office of Naval Research, USA against the Indo-US Programme on "Fundamental Investigation in Advanced Ferrous Alloys". The authors are also grateful to the management of Tata Iron and Steel Co. for providing all research and logistic facilities during the course of this investigation.

REFERENCES

1) T. Gladman and F. B. Pickering: *J. Iron Steel Inst*., **205** (1967), 653.
2) L. J. Cuddy and L. C. Raley: *Metall. Trans. A*., **14A** (1983), 1989.
3) E. J. Palmiere, C. I. Garcia and A. J. DeArdo: *Metall. Trans. A*, **25A** (1994), 277.
4) A. Manohar, D. P. Dunne, T. Chandra and C. R. Killmore: *ISIJ Int*., **36** (1996), 194.
5) M. F. Ashby and K. E. Easterling: *Acta Metall*., **30** (1982), 1969.
6) J. C. Ion, K. E. Easterling and M. F. Ashby: *Acta Metall*., **32** (1984), 1949.
7) I. Anderson and O. Grong: *Acta Metall*., **43** (1995), 2673.
8) M. J. Whelan: *Met. Sci. J*., **3** (1969), 95.
9) J. Ågren: *Scand. J. Metall*., **19** (1990), 2.
10) D. Radaj: Heat Effects of Welding, Springer-Verlag Publication, Heidelberg, (1992), 23.
11) O. Grong: Metallurgical Modelling of Welding, The Institute of Materials, Cambridge, (1997), 301.
12) G. Spanos, R. W. Fonda, R. A. Vandermeer and A. Matuszeski: *Metall. Mater. Trans. A*, **26A** (1995), 3277.
13) W. C. Leslie: The Physical Metallurgy of Steels, McGraw-Hill Publication, New York, (1982), 257.
14) R. C. Hudd, A. Jones and M. N. Kale: *J. Iron Steel. Inst*., **209** (1971), 121.
15) W. Nordberg and B. Aronsson: *J. Iron Steel Inst*., **206** (1968), 1263.
16) T. Gladman: The Physical Metallurgy of Microalloyed Steel, The Institute of Materials, Cambridge, (1997), 110.
17) K. Narita: *Trans. Iron Steel Inst. Jpn*., **15** (1975), 145.

Appendix I. Determination of x in Nb(CxN1-x)

The solubility product k of Nb(C_xN_{1-x}) is given by the equation:

$$\log k = x\log k_1 + (1-x)\log k_2 + x\log x + (1-x)\log(1-x) \quad \text{.....(A-1)}$$

where k_1 and k_2 are the solubility products for NbC and NbN respectively. The temperature dependence of k_1 and k_2 (14) are given as:

$$\log k_1 \text{ (for niobium carbide)} = -7900/T + 3.42 \quad \text{.....(A-2)}$$

$$\log k_2 \text{ (for niobium nitride)} = -8500/T + 2.80 \quad \text{.....(A-3)}$$

where T is the temperature in Kelvin.

Using mass balance equations and stoichiometric ratios[14], the soluble niobium, [Nb], values have been calculated and is given in **Table I**. From [Nb] the fraction of carbide (x) in the carbo-nitride as a function of temperature can be calculated from the mass balance for carbon using the equation:

$$C_T = [C] + C_{NbCN} \quad \text{.....(A-4)}$$

$$C_T = xk_1/[Nb] + x\text{Nb}_{NbCN}(12/93)$$

$$x = C_T/(k_1/[Nb] + 12\text{Nb}_{NbCN}/93) \quad \text{.....(A-5)}$$

where C_T is the total carbon, C_{NbCN} is the carbon content in the carbonitride precipitate, [C] is the carbon content in solution, and Nb_{NbCN} is the Nb content in the carbonitride precipitate.

The values of x in **Table I** show a modest decrease with increasing austenitising temperature. With the given HSLA-

Table I. [Nb] and x as a function of temperature under equilibrium conditions for HSLA-100 steel.

Temp., ^{0}C	950	1000	1050	1100	1115
[Nb]	0.0054	0.0095	0.016	0.026	0.029
x	0.2323	0.228	0.2256	0.224	--

100 chemistry, the carbonitride can therefore be expressed as $NbC_{0.23}N_{0.77}$ for practically all temperatures in the austenite region.

Appendix II. Determination of Dimensionless Supersaturation Value (α)

Using $x=0.23$ and Eq. (A-4) and (A-5), the solubility product k can be expressed as:

$$k=[\mathrm{Nb}][\mathrm{C}]^{x}[\mathrm{N}]^{(1-x)}=\exp(6.236-19254/T) \quad \text{.....(A-6)}$$

The equilibrium concentration of Nb, C_i, at the particle/matrix interface (in mass %) can be estimated from the solubility product Eq. (A-6). If we assume that the carbon and nitrogen concentration at the precipitate–austenite interface is constant and equal to the nominal values of 0.04% and 0.0128% respectively, Eq. (A-6) becomes:

$$C_i(\mathrm{Nb})=\exp(6.236).\ \exp(-19254/T)/[0.04]^{0.23}[0.0128]^{0.77}$$
$$=30705\exp(-19254/T) \quad \text{.....(A-7)}$$

By inserting the atomic weights of Nb, C, N, and $x=0.23$, the concentration of the precipitate is given as:

$$C_p\ (\mathrm{Nb})=[93/\{93+12x+14(1\text{-}x)\}]\ x\ 100\approx 87\%. \quad \text{.....(A-8)}$$

The dimensionless supersaturation, α, can now be written as:

$$\alpha_{\mathrm{Nb}}=C_i(\mathrm{Nb})/C_p(\mathrm{Nb})=353\exp(-19254/T) \quad \text{.....(A-9)}$$